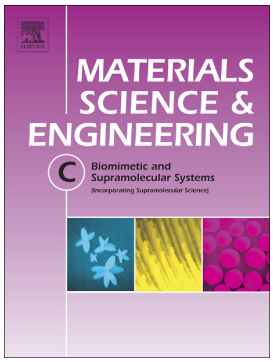


# Magneto-elastic biosensors: Influence of different thiols on pathogen capture efficiency

Márcia Dalla Pozza, André L. Possan, Mariana Roesch-Ely, Frank P. Missell

PII: S0928-4931(16)32290-1
DOI: doi: 10.1016/j.msec.2017.02.091
Reference: MSC 7425

To appear in: *Materials Science & Engineering C*

Received date: 21 November 2016
Revised date: 19 February 2017
Accepted date: 21 February 2017

Please cite this article as: Márcia Dalla Pozza, André L. Possan, Mariana Roesch-Ely, Frank P. Missell , Magneto-elastic biosensors: Influence of different thiols on pathogen capture efficiency. The address for the corresponding author was captured as affiliation for all authors. Please check if appropriate. Msc(2017), doi: 10.1016/j.msec.2017.02.091

# Magneto-elastic biosensors: influence of different thiols on pathogen capture efficiency

Márcia Dalla Pozza[1], André L. Possan[1], Mariana Roesch-Ely[2], Frank P. Missell[1]

1 Centro de Ciências Exatas e Tecnologia, Universidade de Caxias do Sul, Caxias do Sul, RS, Brazil

2 Instituto de Biotecnologia, Universidade de Caxias do Sul, Caxias do Sul, RS, Brazil

## Abstract

Magneto-elastic biosensors have mass sensitivity to biological species, offering reliability and reproducibility in the detection of pathogens such as *Escherichia coli*. In this work, amorphous ribbons of Metglas 2826MB3 were coated with layers of Cr and Au by DC magnetron sputtering and cut to 5 mm x1 mm. The influence of different thiols on captured pathogens was studied. The compounds cystamine (CYS), cysteamine (CYSTE) and mercaptoproprionic acid (MPA) were deposited on Au-covered surfaces, followed by antibodies. The roughness parameters Ra and Rq were determined using atomic force microscopy (AFM) and micrographs from scanning electron microscopy with a field emission gun (FESEM) were also utilized. Biosensors formed with MPA showed an increased efficiency for attracting *E. coli* compared to biosensors with CYS and CYSTE, but large standard deviations were observed, making reproducibility and reliability difficult for that biosensor. Sensors tested with CYSTE showed greater efficiency and a lower detection limit than sensors with CYS. The results indicated that the size of the carbon chain and the terminal grouping influence the effectiveness of immobilization on magneto-elastic biosensors.

## Graphical abstract

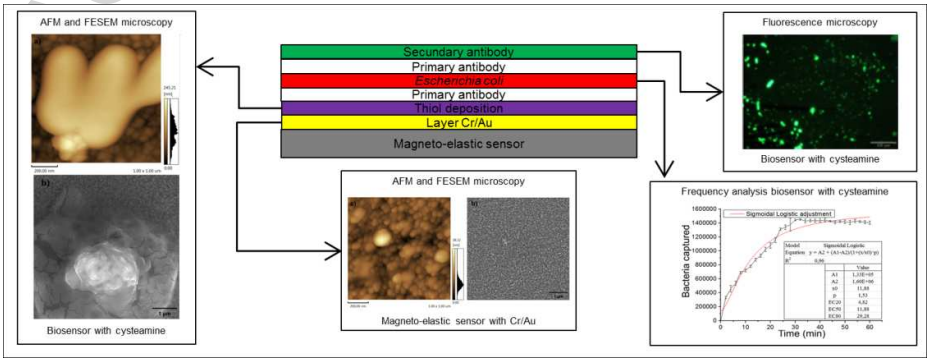

Keywords: immobilization, magneto-elastic, biosensor, resonant frequency, atomic force microscopy, self-assembled monolayer

## 1. Introduction

The Center for Disease Control and Prevention (CDC) estimates that up to 48 million persons become ill every year in the United States due to food-born illnesses, with up to 3000 deaths [1]. In May of this year, General Mills, producer of wheat flours Gold Medal, Wondra and Signature Kitchen, recalled certain lots of their products from the supermarkets because of a relation with the appearance of the *Escherichia coli* bacteria in up to 20 American states [2]. According to the CDC, the average time to diagnose this bacteria is from 1 to 3 days, after obtaining the sample. The detection and rapid quantification are essential for environments which require the control of this pathogen. Magneto-elastic biosensors may be an alternative method for this function since they can be queried remotely in a reliable and secure manner [3].

*E. coli* is a pathogenic agent, which can cause urinary tract infections or infections of the bloodstream. Transmission may occur through the consumption of contaminated food, mainly raw or undercooked meat and milk, as well as through the consumption of raw vegetables. The control of this pathogen is critical in the food and hospital sectors [4].

The detection of pathogens on the functionalized surfaces of magneto elastic biosensors may occur through the formation of self-assembled monolayers (SAM) followed by a specific antibody. The binding of antibodies on a surface modified with a SAM is mediated by crosslinking agents such as EDC and Sulfo-NHS, creating reactive intermediaries and providing the connection with the functional groups of the surface.

Organic compounds with a thiol group at one of its extremities and the other having a carboxyl (R-COOH) or amine ($R\text{-}NH_2$) group may be used for the formation of the SAM. We decided to produce biosensors using the organic compounds cystamine (CYS), cysteamine (CYSTE) as well as mercaptoproprionic acid (MPA) to form the SAM [5].

The formation of the SAM on a gold surface is strongly affected by the nature and roughness of the substrate, by the solvent employed, by the time

and temperature of exposure, by the concentration of the compound, as well as by the length of the thiol molecule utilized. A recent paper [6] has studied the surface functionalization of gold nanoparticles with thiol-based SAMs. Thiol-functionalized gold nanoparticles have proven to be very useful as biosensors [7]. The length of the thiol chain affects the stability of the applied SAM as well as the electron transfer during the formation, thereby influencing the detection sensitivity of the biosensor [8-11].

The cystamine ($C_4H_{12}N_2S_2$) molecule is a dissuphide with two atoms of sulphur (S) in the middle as well as amine groups at each of its extremities [12]. When the bond between the two sulphur atoms is broken, the formation of the SAM may occur. In the case of CYS, two thiols are formed when the S-S bond is broken, leading to a closer coupling of the thiols forming the SAM [13-15].

Cysteamine ($C_2H_7NS$) is the simplest stable aminothiol, having a structure similar to that of cystamine, however with one sulphur atom and a single amine group. The formation of the SAM occurs by breaking the bond with the sulphur and the formation of a bond with the gold substrate.

The molecule of mercaptopropionic acid ($C_2H_6O_2S$) is a short chain thiol with a sulphur and a carboxylic group (COOH) at one of its extremities [14,16]. To form the SAM, the S-H bond is broken, allowing the bonding of the sulphur with the gold surface and promoting an organized and oriented layer [14].

The use of immobilized antibodies on magneto-elastic biosensors, their advantages and disadvantages, has been discussed at some length [17]. Hoping to improve the detection sensitivity of the magneto-elastic biosensor [17,18], this work proposes to analyze the effect of SAM formation (with CYS, CYSTE and MPA) on gold-coated ribbons of Metglas 2826MB3. For this purpose, the functionalized ribbons were exposed to solutions of *E. coli* bacteria and the variations of the ressonant frequency were measured as a function of time with an impedance analyzer. Since the organic compounds employed differ in their structure, the length of their carbon chains and in the terminal group responsible for connecting to antibodies, we might hope to obtain insights into the importance of these factors in determining the sensitivity of the biosensors. The biosensors were also characterized by atomic force microscopy (AFM) in the tapping mode and field emission scanning electron microscopy (FESEM).

## 2. Experiment

The amorphous alloy Metglas 2826MB3, with approximate composition $Fe_{45}Ni_{45}Mo_7B_3$ in weight percent, was furnished by the Metglas Corp. in the form of two inch wide ribbons with a thickness of about 30 μm [19]. The alloy has a saturation magnetostriction ($\lambda_s$) of = ppm, a density of ρ= 7900 $kg.m^{-3}$, a Young modulus E of approximately 105 GPa and a Poisson ratio of σ= 0.33 [20,21]. The ribbons were first mechanically polished on both sides using a Struers Tegramin 20 polishing system with 0.05 μm alumina and demineralized water. After reducing the thickness to about 15 μm, layers of Cr (~128 nm) and Au (~117 nm) were deposited by DC magnetron sputtering [22]. The Cr layer was added to improve the adherence of the gold layer. Previously [22] an elemental analysis of the films using Rutherford backscattering spectroscopy was reported. A micro-dicing saw was then used to cut sensor substrates with dimensions 5 mm x 1 mm x 0.015 mm.

Atomic force microscopy (AFM) was performed using the Shimadzu Scanning Probe Microscope SPM 9700 in the tapping mode with NCHR-10 silicon tips. All parameters were adjusted to permit scans over an area of 1 $\mu m^2$. Average roughness values were calculated using the system software and the averaging was done over three areas of 1 $\mu m^2$ and the results were averaged. Field emission scanning electron microscopy (FESEM) was performed using a TESCAN model MIRA 3.

Cystamine dihydrochloride (≥98%), cysteamine (≥98%) and 3-mercaptopropionic acid (≥99%) were purchased from Sigma Aldrich. The reagents *N*-(3-Dimethylaminopropyl)-*N′*-ethylcarbodiimide (EDC) and *N*-Hydroxysulfosuccinimide (Sulfo-NHS) used for the dilution and activation of the antibodies were also acquired from Sigma Aldrich. The preparation of each compound studied (CYS, CYSTE, or MPA) for the formation of the SAM proceeded by dissolving the material in ethanol at a concentration of 20 mM, followed by agitating at 1700 rpm for about 24 hours at room temperature. After the deposition of the material, the sensor was washed with the solvent in order to remove molecules that are not adhering well and transferred to a micro reaction tube (Eppendorf).

The primary antibody anti-*E. coli* ab137967, acquired from ABCAM, was diluted to a concentration of 0.02 mg.mL$^{-1}$ with PBS (pH 7.4). For the CYS and CYSTE sensors we added EDC 20 mM in the proportion 1:100 with the antibody and incubated the result for 2 hours at a temperature of 37 ºC. For the MPA sensors, we added EDC 15 mM and Sulfo-NHS 35 mM for two hours at room temperature and later the diluted antibodies for 2 hours at 37 ºC. After the application of the antibody, the biosensor was washed with PBS (pH 7.4) in order to remove non-specific bonds. For analysis using the fluorescence microscope, the secondary antibody goat anti-rabbit IgG H&L Alexa Fluor 488, also acquired from ABCAM, was applied after being diluted to a concentration of 0.008 mg.mL-1 with PBS (pH 7.4) [24-26].

The *E. coli* bacteria were transferred to a Petri dish with semisolid Luria Bertani (LB) medium from the original sample [27]. After the growth period had passed (24 h at 37 ºC), a single colony forming unit (CFU) was used for inoculation and growth in 100 mL of liquid LB medium. A series of dilutions were carried out using PBS (pH 7.4), starting from the concentrated bacteria. Initially 0.9 mL of the PBS solution and 0.1 mL of the bacteria-containing solution were mixed and this process was repeated until a dilution of $10^{-6}$ was attained, permitting a direct counting of the CFU in the semi-solid medium. For each analysis, new suspensions of bacteria were produced. The contamination of the biosensors was carried out with an *E. coli* concentration of about $10^{9}$ CFU.mL$^{-1}$.

The shifts in the resonant frequencies were measured as a function of time for 60 minutes using an Agilent E5061B impedance analyzer. Measurements were taken automatically at intervals of 2 minutes. Further details about the resonant frequency measurements have been given previously [22,23].

## 3. Results and Discussion

### 3.1 Surface characterization of the bare magneto-elastic sensors

As mentioned previously, sensor surfaces were covered with layers of Cr and Au after polishing, using DC magnetron sputtering. The sensor surfaces were examined using atomic force microscopy in the tapping mode. A typical

result is shown in Fig. 1a. This surface presented $R_a$ = 2.8±0.1 nm and $R_q$ = 3.5±0.1 nm. The figure on the right hand side of the AFM image represents $R_t$ and has a value of 38.3 nm. The $R_t$ parameter, also known as $R_{max}$, is defined as the distance between the highest peak and the lowest valley [28]. The AFM image shows rounded grains with sizes ranging from 10 to 200 nm. The morphology of the Au particles varies with the preparation method and with the observation conditions [29]. On the right hand side of Figure 1 we present the FESEM image of the Au-covered sensor surface (Fig. 1b).

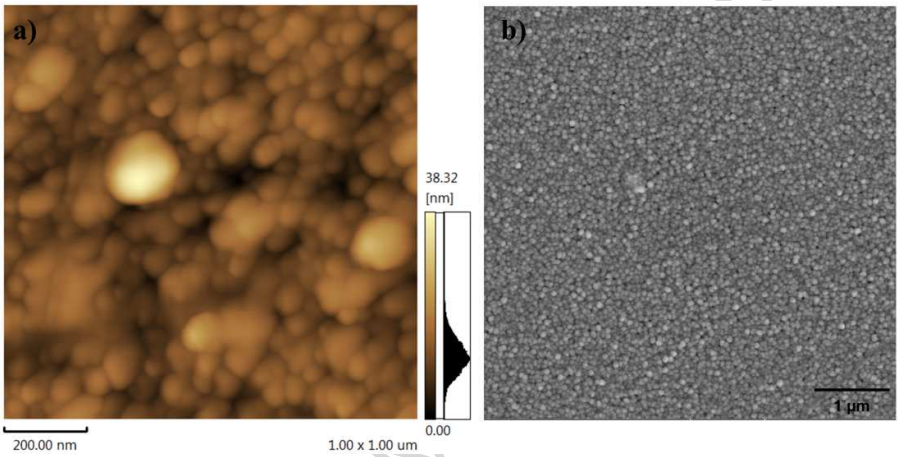


**Figure 1.** a) Atomic force microscope image b) FESEM micrograph of magneto elastic sensor substrate covered with Cr/Au by sputtering.

## 3.2 Evaluation of the CYS magneto elastic biosensor

A solution of 20 mM of CYS was applied to the Au surface for 24 hours at room temperature in order to form the SAM. After the time had passed for the surface formation, the surface was again analyzed using the AFM and the FESEM. The results are shown in Fig. 2.

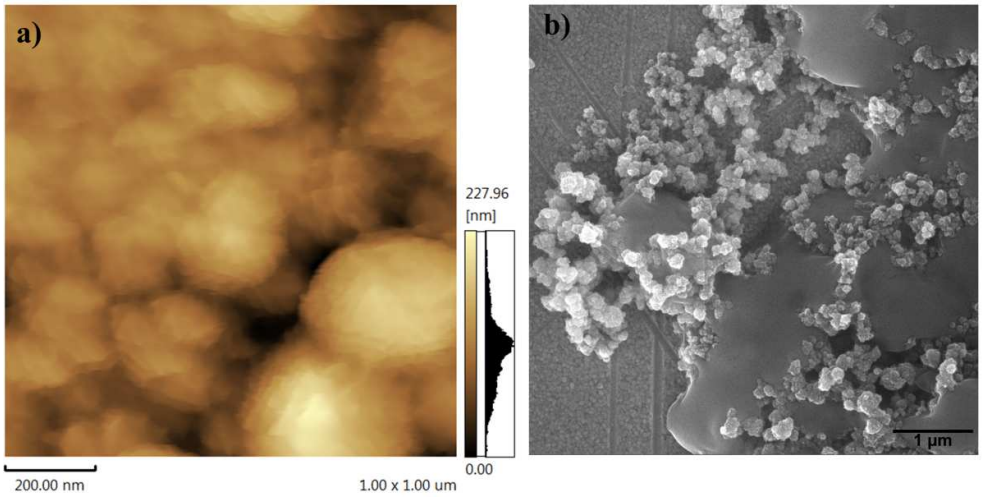


**Figure 2.** a) Atomic force microscope image b) FESEM micrograph of the SAM with CYS on the Au surface of a magneto elastic sensor.

From the AFM image it was possible to calculate the surface roughness: $R_a$= 29±6 nm and $R_q$=34±4 nm. These values are about 10 times larger than those encountered after deposition of Au on the sensor substrate and leave no doubt that the sensor surface has been modified. The parameter Rq represents the standard deviation of the peak heights on the surface [28], which is comparable to the $R_a$ value. The maximum value of $R_t$ in this case is 228 nm, again nearly 10 times the $R_a$ value.

In the FESEM image on the right hand side of Figure 2 (Fig. 2b) one can see the presence of a dense layer of CYS which takes the form of an agglomerate. The gold layer of the sensor can also be seen in this image, indicating that total coverage of the substrate did not occur. Scratches associated with the polishing process are also visible. Additionally, an improvement in the sensor surface may increase the density of the SAM during its formation [10,22].

After applying the CYS, antibodies and bacteria solution were applied and five biosensors were tested under the same conditions. Values of $\Delta$f were collected, together with results for the reference sensor. At the initial time, the value of resonance frequency was recorded and taken as zero. Frequency shifts were then measured as a function of time. These data are shown in Fig. 3a. Now it is possible to estimate the number of bacteria captured using the expression for the mass sensitivity of the biosensor (Eq. 1 below). We take the

mass of a single *E. coli* bacteria to be $1x10^{-15}$ kg. Then the equation for $S_m$ may be used to estimate the number of bacteria by dividing the average values of $\Delta f$ by the sensitivity $S_m$ and the bacteria mass [19,22]. One thus obtains an estimate of the number of bacteria captured by the biosensor.

$$S_m = -\frac{5}{4\rho L^3 t}\sqrt{\frac{E}{\rho(1-\sigma)}} \tag{1}$$

Figure 3b shows the average values of Δf converted into the number of bacteria captured by the biosensor as a function of time, as well as a curve representing the Sigmoidal Logistic of these results. The parameters A1, A2, xo and p are respectively, the initial number of bacteria, the final number of bacteria, the time necessary to attain the midpoint of the slope, and power associated with the slope. This analysis furnishes the percentages of bacterial capture for a non-linear curve, represented by the points EC20, EC50 and EC80 [30,31].

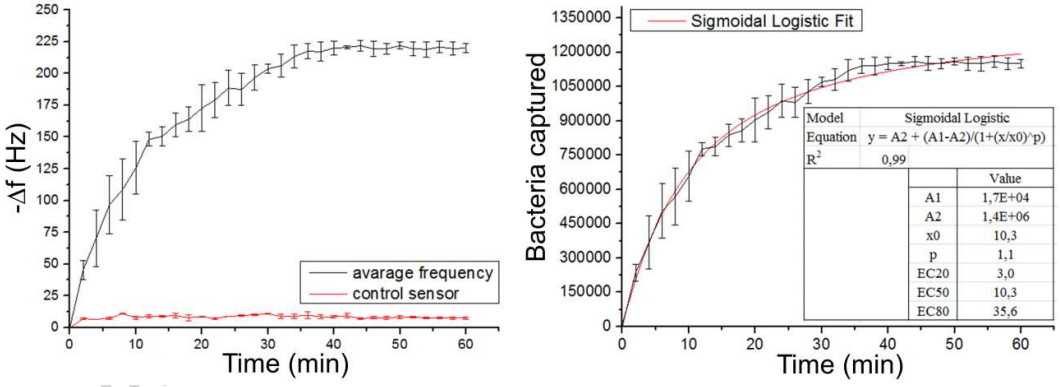


**Figure 3**. a) Average variation of the resonant frequency of 5 biosensors prepared with CYS together with the reference sensor b) estimated number of bacteria captured for biosensors prepared with CYS as a function of time showing the Sigmoidal Logistic Fit.

The data obtained show that the capture of bacteria increases up to about 30 minutes and thereafter saturates. This may be related to the distribution of the adherence points. The maximum variation of the resonant frequency was 221 Hz. We verified also that larger values of the standard

deviation for the initial times in relation to the final times could be explained in terms of the distribution of bacteria and the variation of the connections with the antibodies. One can observe that the maximum number of bacteria captured is around $1.3x10^6$, corresponding to a capture time of about 30 minutes, corroborating the results obtained by [22].

3.3 Evaluation of the MPA biosensor

The use of mercaptoproprionic acid to build the SAM of the biosensor on the sputtered Au layer was also investigated using AFM e FESEM. Results are shown in Figure 4.

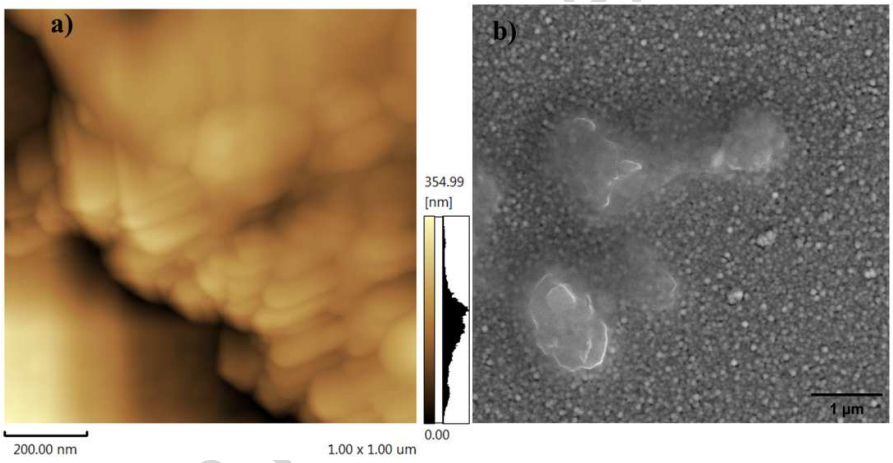


**Figure 4.** a) Atomic force microscope image b) FESEM micrograph of SAM prepared with MPA on Au surface of sensor substrate.

In Figure 4a, it is possible to see an accentuated contrast between regions, where the bright and dark regions have different thicknesses. The surface topography of the sensor with MPA also shows an increase in the parameters $R_a$ and $R_q$ compared with the Au-covered surface. We found $R_a$ = 47±6 nm and $R_q$ = 60±3 nm, indicating a modification of the surface with the deposition of the MPA. In this case $R_t$ = 355 nm. The surface with MPA presented larger values of $R_a$ and $R_q$ when compared with the CYS-covered surface. However, the larger difference between the $R_a$ and $R_q$ values are indicative of a bit scattered layer.

In the FESEM micrograph (Fig. 4b) one does not observe platelets as in the case of the surface with CYS, but rather dispersed agglomerates and the

surface of the sensor substrate is also visible. These results suggest only traces of the monolayer are present on the substrate.

After the deposition of the MPA, the protocol for applying the antibodies and bacteria solution was followed. Five biosensors were then tested under the same conditions. Values of ∆f were collected together with values for the reference sensor and are presented in Figure 5a. As was done previously, the frequency variation data were converted into the number of bacteria captured as illustrated in Figure 6b and the Sigmoidal Logistic fit was also carried out.

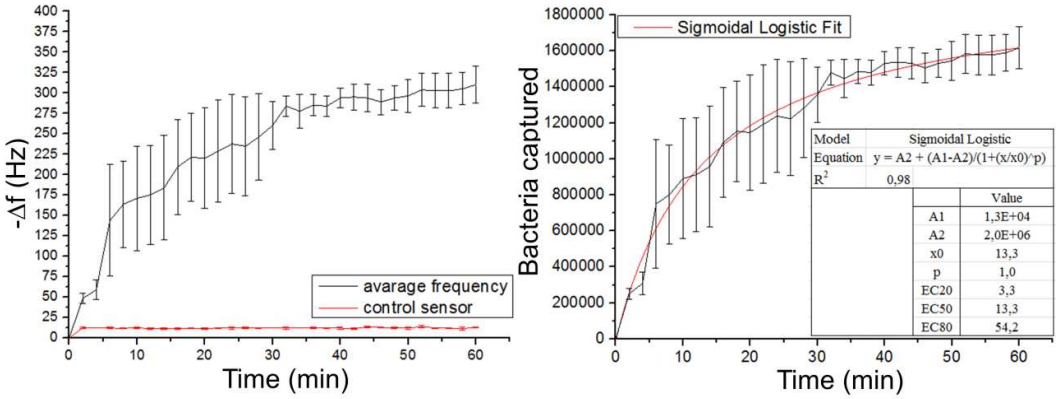


**Figure 5.** a) Average variation of the resonant frequency of 5 biosensors prepared with MPA together with the reference sensor b) estimated number of bacteria captured for biosensor prepared with MPA as a function of time showing the Sigmoidal Logistic fit.

We observed a large variation in the ∆f values up to the time of saturation (about 35 minutes), resulting in large values for the standard deviation and low reproducibility. Comparing biosensors made by deposition of CYS or MPA, the latter apparently showed a greater capacity for capturing bacteria, the frequency difference being about 89 Hz in a total of 310 Hz, however with large values of the standard deviation. It is estimated that the maximum number of bacteria which could be captured by our biosensor is about $1.9 \times 10^6$.

The SAM of a bit scattered as well as variations in the organization of the antibodies might be collaborating to induce a lack of reproducibility in the biosensors terminating in COOH. There is some evidence that surfaces with SAM ending in $NH_2$ possess more active sites for fixing antibodies than surfaces terminating in COOH. This may be due to a better orientation of antibodies on the surface modified with $NH_2$ than COOH [32].

3.4 Evaluation of the CYSTE biosensor

The formation of the SAM of cysteamine on the magneto-elastic sensor substrate covered with Cr/Au was evaluated with the AFM and FESEM, as illustrated in Figure 6.

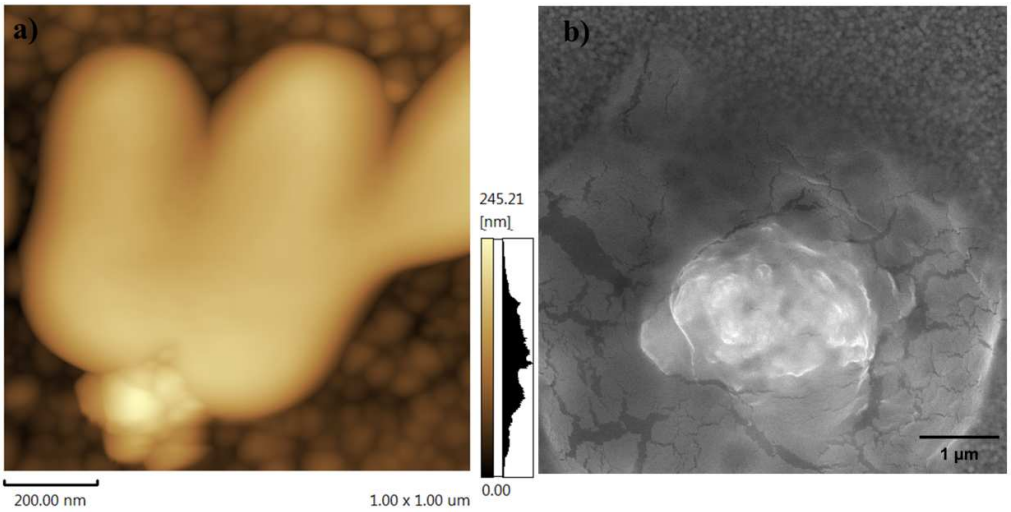


**Figure 6.** a) Atomic force microscopy image b) FESEM micrograph of the SAM prepared with CYSTE on the Au surface of the sensor substrate.

The atomic force microscopy of the surface with cysteamine furnished values $R_a$=20±1 nm and $R_q$=26±2 nm indicating that the surface of the Au-covered sensor was modified by the monolayer. Here, $R_t$ is 245 nm. In this case, the values of $R_a$ and $R_q$ are close, suggesting that the surface presents few irregularities. The dark regions correspond to the Au-covered surface of the sensor, while the clear regions are evidence of the applied CYSTE.

One can note in the FESEM micrographs that the deposition of CYSTE also did not give rise to complete coverage of the sensor surface. However, the continuity of the deposited film can be noted from the fact that the empty spaces have been reduced, favoring the construction of the magneto elastic biosensor.

Using the surfaces modified with CYSTE, the antibodies and bacteria solution were applied and five biosensors were tested under the same conditions, with the results given in Figure 7a. The data for the frequency variations were also converted into estimates of the number of bacteria captured, shown in Figure 7b. The data were fitted to the Sigmoidal Logistic function as shown.

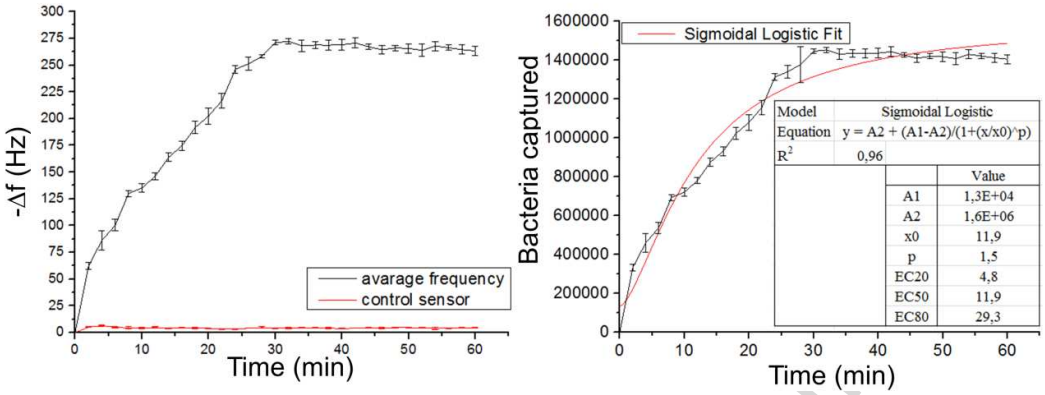


**Figure 7**. a) Average variation of the resonant frequency for 5 biosensors prepared with CYSTE together with the reference sensor b) estimated number of bacteria captured for biosensor prepared with CYSTE as a function of time with Sigmoidal Logistic fit.

The biosensors made with CYSTE also exhibited saturation after about 35 minutes. Low values of the standard deviation are observed, perhaps indicating a scattered layer of CYSTE on the substrate, favoring the connection of the antibodies via the terminal amine groups. The maximum resonant frequency variation was about 272 Hz, corresponding to the estimated capture of ~$1.6.10^6$ bacteria. This value was inferior to that observed on biosensors produced with MPA and greater value than the biosensors with CYS.

In spite of the fact that both MPA and CYSTE are short-chain thiols, they differ in terms of the terminal group. The author of [10] suggests that a monolayer of CYSTE is more stable because more energy is necessary to remove it from the metal and the terminal amine group facilitates the transfer of electrons during the formation of the SAM. That author also claims that the breaking of the S-S bond, in the case of CYS, can cause irregularities in the formation of SAM.

### 3.5 Fluorescence microscopy

To visualize the *E. coli* bacteria on the surface of the biossensor, we used fluorescence microscopy. Utilizing the fluorescence microscope with appropriate filters it is possible to verify the presence of bacteria, which are linked to the secondary antibody and consequently to the first antibody, since

the secondary antibody is marked with fluorescein (Alexa Fluor 488). The results are shown in Figure 8.

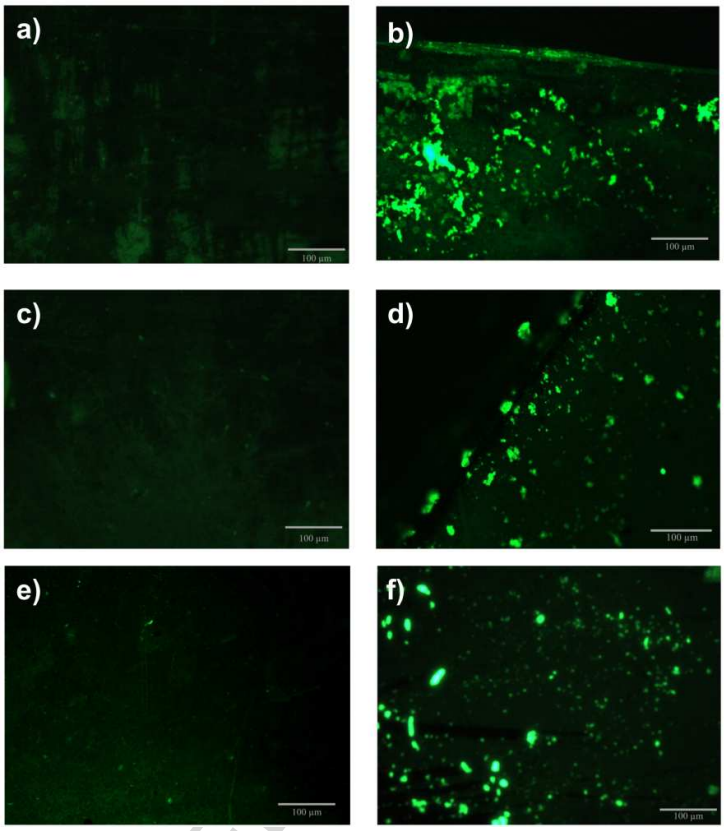


**Figure 8**. Fluorescence micrograph a) reference biosensor with CYS and b) captured bacteria on biosensor surface with CYS deposition c) reference biosensor with MPA and d) captured bacteria on biosensor surface with MPA deposition e) reference biosensor with CYSTE and f) captured bacteria on biosensor surface with CYSTE deposition.

In Figure 8b, one can observe large concentrations of bacteria in certain regions of the biosensor, forming agglomerates which can be distinguished by their light green color. The dark regions indicate the absence of bacteria which may be related to the absence of the CYS in that region of the sensor.

From the micrographs obtained from fluorescence microscopy of biosensors with MPA (Figs. 8c and 8d), we verify that the distribution of bacteria is less uniform than for the case discussed previously and that several regions show a complete absence of bacteria. This evidence suggests a certain variability in the biosensors produced using MPA, even though they seem to capture more bacteria than those produced with CYS.

The fluorescence images of biosensors employing CYSTE (Fig. 8e and 8f) also show regions without bacteria, however there is a greater dispersion of the bacteria over the surface and few agglomerates are observed. This may be the reason for the better performance of these sensors.

3.5 Detection limits

The detection limit gives the minimum detectable concentration of bacteria which can be identified by the magneto-elastic biosensors. To estimate the detection limit of the biosensors we calculated the standard deviation ($S_{med}$) of the difference between the mean error of bacterial capture and the reference biosensor [33]. The results are shown in Table 1. It is worth mentioning that this definition of the detection limit [33] is different from that used by some authors. For example, Guntupalli *et al*. [34] used magneto-elastic biosensors to detect *Salmonella typhimurium*, obtaining a detection limit of 5 x $10^3$ cfu/ml by extrapolating their results to lower bacterial concentrations. However, the colony-forming unit (cfu) is relatively difficult to determine and its value may differ from laboratory to laboratory. For this reason we have preferred the definition of [33].

**Table 1**. Detection limits of bacteria for the biosensors tested with CYS, MPA and CYSTE.

| | Biosensor with CYS | Biosensor with MPA | Biosensor with CYSTE |
|---|---|---|---|
| $S_{med}$ (Hz) | 9.0 | 33.3 | 4.1 |
| Detection limit (bacteria.mL$^{-1}$) [a] | 4.7x10$^4$ | 1.7x10$^5$ | 2.1x10$^4$ |
| Detection limit (ng.mL$^{-1}$) [a] | 46.9 | 173.0 | 21.7 |

[a] [33]

The biosensor produced with MPA presented the highest detection limit, followed by CYS and CYSTE. Again the biosensor with CYSTE showed the best results compared with the other compounds considered, thereby confirming interest in using this material for the fabrication of the sensor.

The efficiency of the biosensors could be estimated from the fact that the estimated sensitivity for sensors with the dimensions of 5 mm x 1 mm is 376

Hz [22]. Table 2 presents the estimated efficiency for the biosensors tested considering the theoretical value of 376 Hz as the maximum variation of resonant frequency which might be encountered. The efficiency was then calculated as the observed frequency shift divided by the theoretical value of 376 Hz.

**Table 2**. Estimated efficiency for the biosensors with CYS, MPA and CYSTE.

| | $\Delta f_{est}$ (Hz) | $\Delta f_{max}$ (Hz) | Efficiency (%) |
|---|---|---|---|
| Biosensors with CYS | 376 | 221 | 59 |
| Biosensors with MPA | | 310 | 82 |
| Biosensors with CYSTE | | 272 | 72 |

The biosensor whose surface had been modified by MPA showed the greatest efficiency in relation to others. However, as discussed previously, these biosensors did not present reliability and showed a certain variability in the values measured. This resulted in a greater standard deviation and a higher detection limit. On the other hand, biosensors prepared with CYSTE showed a good efficiency in detecting *E. coli* bacteria on the surface of magneto-elastic sensors.

3.6 Sigmoidal logistic and variance analysis

Table 3 presents results obtained for the capture of the bacteria from Sigmoidal Logistic fits for the three compounds studied.

**Table 3**. Capture of bacteria from Sigmoidal Logistic fits to data obtained from biosensors with CYS, MPA and CYSTE. EC X is the capture rate when the curve of number of bacteria vs. time reaches X percent of its saturation value.

| | Capture of bacteria with different thiols | | |
|---|---|---|---|
| | CYS | MPA | CYSTE |
| EC 20 | $3.0x10^5$ | $2.9x10^5$ | $4.9x10^5$ |

| | | | |
|---|---|---|---|
| EC 50 | $6.7x10^5$ | $9.4x10^5$ | $7.8x10^5$ |
| EC 80 | $1.1x10^6$ | $1.6x10^6$ | $1.4x10^6$ |
| Maximum capture | $1.4x10^6$ | $2.0x10^6$ | $1.6x10^6$ |

In all cases one observes a increase in the capture as time goes on, indicating a tendency to saturation. On the surface with MPA, the point EC80 occurs after 54 minutes, different than for the surfaces with CYS and CYSTE where this point occurs after approximately 35 and 30 minutes respectively. This result indicates an improvement in the surface with CYSTE when compared with the other compounds studied. For all of the cases studied, the coefficient ($R^2$) presented superior values to 0.95, showing that the mathematical model is appropriate to represent the data. The mathematical polynomial fit also could be applied, however we chose Sigmoidal logistic due to data percentages positions provided by this model.

The analysis of variance (ANOVA) was used to evaluate the significance of the interactions between the groups. The ANOVA analysis provides the sum of squares (SS), degrees of freedom (DF), squared mean (SM), $F_{calculated}$, P value and $F_{critical}$. To test the hypothesis relative to the effects of the groups, the F Test was used, comparing $F_{calculated}$ with $F_{critical}$. If the calculated value is greater than the critical value there are significant differences between the groups caused by the controllable factor of the study. Another way to evaluate significant differences is through the P value. If the P value is lower than or equal to the significance level (α), the differences between the groups will also be significant. Table 4 shows the ANOVA analysis of the experimental data obtained with the Sigmoidal Logistic fit for the number of bacteria captured on the surface of the magneto elastic biosensor with each different thiol studied [33,35,36].

**Table 4**. ANOVA analysis of the experimental data obtained with the *Sigmoidal Logistic* fit for the number of bacteria captured on the surface of the magneto elastic biosensor with each different thiol studied.

| Sources of variation | SS | DF | SM | $F_{calculated}$ | P Value | $F_{critical}$ |
|---|---|---|---|---|---|---|
| Factor A* | $3.0x10^{12}$ | 3 | $1.0x10^{12}$ | 44.2 | 0.00 | 3.2 |
| Factor B** | $2.2x10^{11}$ | 2 | $1.1x10^{11}$ | 4.8 | 0.05 | 3.4 |

| | | | |
|---|---|---|---|
| Error | $1.3x10^{11}$ | 6 | $2.3x10^{10}$ |
| Total | $3.4x10^{12}$ | 11 | |

*EC values

**Different thiols

It is observed in Table 4 that the values of $F_{calculated}$ were higher in comparison with $F_{critical}$ and the P value also proved to be lower than the level of significance (α = 0.1). Thus, with 90% significance it is possible to affirm that there are significant differences between the groups, caused by the controllable factor of the study, that is, by the different thiol used. The multiple range test was also performed by the Duncan method, as shown in Table 5 [35,36]. The difference will be significant if the means comparison is greater than the decision limit (Dl).

**Table 5**. Multiple range test of statistical data obtained with magneto-elastic biosensors

| Factor A Dl: $3.0x10^5$ | | | Factor B Dl: $2.6x10^5$ | | |
|---|---|---|---|---|---|
| | Range | Comparison | | Range | Comparison |
| EC20 | $3.5x10^5$ | $4.4x10^5$ | | | |
| EC50 | $7.9x10^5$ | $5.7x10^5$ | CYS | $8.6x10^5$ | $2.0x10^5$ |
| EC80 | $1.3x10^6$ | $2.8x10^5$ | CYSTE | $1.0x10^6$ | $1.3x10^5$ |
| Maximum | $1.6x10^6$ | $1.6x10^6$ | MPA | $1.2x10^6$ | $3.3x10^5$ |

The data presented in Table 5 indicate that, in the case of EC values (Factor A), the difference is significant only in EC20 and EC50, with no significant difference between point EC 80 and maximum point. The data obtained with the different thiols (Factor B) indicate that there is no significant difference between the use of CYS and CYSTE, the difference occurs only with the use of MPA.

The statistical analysis showed that the use of CYS and CYSTE is indifferent, but it is worth mentioning that, the use of CYSTE showed higher bacteria capture, a lower detection limit and a greater efficiency in relation to CYS. The use of CYSTE was also shown to be more stable compared to the

other thiols tested, since the mean standard deviation for this compound was 4.2 Hz, whereas for CYS and MPA it was 9.1 Hz and 33.1 Hz, respectively.

## 4. Conclusions

The performance of the magneto elastic biosensors for the detection of *E. coli* was investigated for the deposition of different organic compounds forming the SAM. In fact, the FESEM images revealed that the organic compounds formed agglomerates on the sensor surfaces which bore little resemblance to monolayers. Biosensors formed with MPA proved better at attracting bacteria than biosensors with CYS and CYSTE, but large standard deviation values were observed, indicating a low reproducibility and reliability of the biosensor. The large standard deviation values ultimately resulted in higher detection limits for this thiol. Biosensors produced with CYSTE showed higher efficiency and lower detection limit than the biosensors tested with CYS, indicating an improvement in the use of this compound. Fluorescence microscopy indicates that CYSTE sensors have a more uniform distribution of bacteria than the others, consistent with the FESEM images. The results for the detection of *E. coli* indicate that the size of the carbon chain and the terminal grouping influence the effectiveness of the immobilization on the magneto-elastic biosensors, possibly by giving rise to a more uniform layer on the sensor surface.

## 5. Acknowledgments

The authors wish to thank A.D. Santos and LcMic of UCS for assistance in the development this work. There were also useful discussions with E. Chinaglia. This work was supported by Project 447777/2014-9 from Conselho Nacional de Desenvolvimento Científico e Tecnológico (CNPq). MDP was supported by CNPq and FPM received partial support from this organization. ALP was supported by CAPES.

## 6. References

[1] Food borne burden. Estimates of food borne illness in the United States, downloaded on September 15, 2016 from http:// www.cdc.gov/foodborneburden/index.html.

[2] The Wall Street Journal. Gold Medal, Gold Medal Wondra and Signature Kitchens flour recalled due to possible E. coli O121 contamination, May 31, 2016. downloaded on July 26, 2016 from http://www.wsj.com/articles/PR-CO-20160531-911562>.

[3] S. Horikawa, Low-cost, rapid, sensitive detection of pathogenic bacteria using phage-based magneto-elastic biosensors. (Ph.D thesis, Auburn University), 166 pp., 2013.

[4] M. I. Morosini, Current issues in multi drug resistant gram negatives – *Escherichia coli*. In: 14th International Congress on Infectious Diseases (ICID), 2010, Florida, USA.

[5] X. L. Su, Y. Li. A self-assembled monolayer based piezoelectric immunosensor for rapid detection of *Escherichia coli* O157:H7. Biosens. Bioelectron. 19 (2004) 563-574.

[6] V. Spampinato, M. A. Parracino, R. La Spina, F. Rossi, G. Ceccone, Surface analysis of gold nanoparticles functionalized with thiol-modified glucose SAMs for biosensor applications, Front. Chem 29 February 2016 https://doi.org/10.3389/fchem.2016.00008

[7] P. G. Sutariya, A. Pandya, A. Lodha, S. K. Menon, A simple and rapid creatinine sensing via DLS selectivity, using calix[4]arene thiol functionalized gold nanoparticles, Talanta 147 (2016) 590-597.

[8] J. Cancino, S. Machado, Microelectrode array in mixed alkanethiol self-assembled monolayers: Electrochemical studies. Electrochim. Acta 72 (2012) 108-113.

[9] R. Radhakrishnan, M. Pali, H. J. Lee, R. Lee, I. I. Suni, Impedance biosensor incorporating a carboxylate-terminated bidentate thiol for antibody immobilization, J. Electrochem. Soc. 163 (2016) B125-B130.

[10] R. K. Mendes, Investigação dos efeitos dos procedimentos de imobilização em monocamadas auto-organizadas da enzima peroxidase no desenvolvimento de um biossensor (Portuguese). (Ph.D. thesis, Universidade Estadual de Campinas) 128 pp., 2006.

[11] S. K. Moccelini, Sensores modificados com monocamadas auto-organizadas de tióis para determinação de dopamina, tiodicarbe e catequina

(Portuguese). (Ph.D.thesis, Universidade Federal de Santa Catarina) 130 pp, 2011.

[12] M. Braiek, K. B. Rokbani, A. Choudra, B. Mrabet, A. Bakhrouf, A. Maaref, N. Renault, Eletrochemical immunosensor for detection of *Staphylococcus aureus* bacteria based on immobilization of antibodies on self-assembled monolayers-functionalized gold electrode. Biosensors 2 (2012) 417-426.

[13] A. Galli, Desenvolvimento de um biossensor bienzimático imobilizado sobre monocamadas auto-organizadas para determinação de açúcares em alimentos (Portuguese). (Ph.D. thesis, Universidade de São Paulo, São Carlos) 143 pp, 2009.

[14] R. Mossanha, Preparação, caracterização e estudos eletroquímicos de eletrodos modificados com diferentes monocamadas auto-organizadas (Portuguese). (Master dissertation - Universidade Estadual de Ponta Grossa) 160 pp, 2011.

[15] M. Wirde, U. Gelius, Self-assembled monolayers of cystamine and cysteamine on gold studied by XPS and voltammetry. Langmuir.15 (1999) 6370-6378.

[16] A. T. S. Neto. Marcação de antígenos eritrocitários do sistema ABO com nanopartículas fluorescentes de semicondutores (Portuguese). (Master dissertation - Universidade Federal de Pernambuco) 86 pp, 2012.

[17] C. Menti, J. A. P. Henriques, F. P. Missell, M. Roesch-Ely, Antibody-based magneto-elastic biosensors: potential devices for detection of pathogens and associated toxins, Appl. Microbiol. Biotechnol. 100 (2016) 6149-6163.

[18] C. Menti, M. Beltrami, M.D. Pozza, S. T. Martins, J.A.P. Henriques, A. D. Santos, F. P. Missell, M. Roesch-Ely, Effect of distinct antibody immobilization strategies on the analytical performance of a magneto-elastic immunosensor for *Staphylococcus aureus* detection, submitted.

[19] Metglas® 2826MB Magnetic Alloy. Magnetic Materials, Metglas Products, downloaded on March 23, 2015 from <http://www.metglas.com/products/magnetic_materials/>.

[20] C. Liang, S. Morshed, B. C. Prorok, Correction for longitudinal mode vibration in thin slender beams. Appl. Phys. Lett., 90 (2007) 221912.

[21] W. Shen, L. Mathison, V. Petrenko, B. Chin, Design and characterization of a magneto-elastic sensor for the detection of biological agents. J. Phys. D: Appl. Phys 43 (2010) 015004.

[22] A. L. Possan, C. Menti, M. Beltrami, A. D. Santos, M. Roesch-Ely, F. P. Missell. Effect of surface roughness on performance of magnetoelastic

biosensor for the detection of *Escherichia coli*. Mater Sci Eng **C** Mater Biol Appl. 58 (2016) 541-547.

[23] C. Menti, M. Beltrami, A. L. Possan, S. T. Martins, J. A. P. Henriques, A. D. Santos, F. P. Missell, M. Roesch-Ely, Biocompatibility and degradation of gold-covered magneto-elastic biosensors exposed to cell culture, Colloids Surf., B 143 (2016) 111-117.

[24] J. C. Ball, G. P. Libby, L. G. Bachas. Covalent immobilization of β-galactosidase onto a gold-coated magnetoelastic transducer via a self-assembled monolayer: Toward a magnetoelastic biossensor. Anal. Chem. 75 (2003) 6932-6937.

[25] G. T. Hermanson, Chapter 1 - Functional Targets. In: G. T. Hermanson (Ed.). Bioconjugate Techniques (Second Edition**)**. (New York: Academic Press, 2008).

[26] G. T. Hermanson, Chapter 3 - Zero-Length Crosslinkers. In: G. T. Hermanson (Ed.). Bioconjugate Techniques (Second Edition**)**. (New York: Academic Press, 2008).

[27] G. Sezenov, D. J. Petit, R. Ari, *Escherichia coli* physiology in Luria-Bertani broth. J. Bacteriol. 189 (2007) 8746–8749.

[28] E. S. Gadelmawla, M. M. Koura, T. M. A. Maksoud, I. M. Elewa, H. H. Soliman, Roughness parameters. J. Mater. Process. Tech.123 (2002) 133-145.

[29] J. A. Fischer, Estudo da formação de monocamadas auto-organizadas de tióis sobre Au (111) (Portuguese). (Master dissertation – Universidade Federal de Santa Catarina) 83 pp. 2011.

[30] S. Gadagkar, G. B. Call, Computational tools for fitting the hill equation to dose response curves. J Pharmacol Toxicol Methods 71 (2015) 68-76.

[31] P. N. Mendes, Ajuste dos modelos Gompertz e Logístico na descrição das curvas de crescimento de tomates: uma abordagem baynesiana (Portuguese). (Ph.D. thesis - Universidade Federal de Lavras) 83pp, 2011.

[32] S. Chen. L. Liu, J. Zhou, S. Jiang, Controlling antibody orientation on charged self-assembled monolayer,. Langmuir 19 (2003) 2859-2864.

[33] D. A. Skoog et al., Fundamentals of analytical chemistry. 9.ed. (Belmont, USA: Cengage Learning, 2014).

[34] R. Guntupalli, R. S. Lahshmanan, J. Hu, T. S. Huang, J. M. Barbaree, V. Vodyanoy, B. A. Chin, Rapid and sensitive magnetoelastic biosensors for the detection of *Salmonella Typhimurium* in a mixed microbial population, J. Microbiol. Methods 70 (2007) 112–118.

[35] J. U. Ani, N. J. N. Nnaji, O. D. Onukwuli, C. O. B Okoyea, Nephelometric and functional parameters response of coagulation for the purification of industrial wastewater using *Detarium microcarpum*. J. Hazard. Mater. 243 (2012) 59-66.

[36] S. Vieira. Análise de variância: (Anova).(São Paulo, Atlas, 2006).

## 7. Vitae

Engª Márcia Dalla Pozza was born in Bento Gonçalves, RS, Brazil and received a degree in Chemical Engineering from the University of Caxias do Sul (UCS) in 2014. Her research interests include magneto-elastic biosensors and atomic force microscopy.

Msc. André Luís Possan was born at Garibaldi, Rio Grande do Sul – Brasil. He received a degree in Chemical Engineering at the University of Caxias do Sul (UCS), 2013, as well as a master's degree in Processes and Technologies at the same university in 2015. Currently, the focus of his Ph.D. research, in the Material Science and Engineering Program, is the study of biomaterials and chemical products for building and monitoring SAMs as well as testing and discovering new forms to bind pathogens on biosensors and bioelectrodes with efficiency.

Mariana Roesch Ely has a Ph.D in Dental Medicine from the University of Heidelberg, Germany. Currently she is a lecturer and researcher at the Biotechnology Institute at University of Caxias do Sul, Brazil. Her research fields are on cell and molecular biology, with focus on proteomics, cell signalling, drug delivery systems and discovery of

Frank P. Missell has a Ph.D in Physics from Massachusetts Institute of Technology. He was the coordinator of the Magnetic Materials Laboratory at the University of São Paulo, Brazil. He is currently a professor at the University of Caxias do Sul where he is interested in magnetoelastic sensors and magnetic materials.

Highlights

-Different thiols were used to capture pathogens on magneto-elastic biosensors.
-Atomic force microscopy (AFM) and scanning electron microscopy with field emission gun (FESEM) were utilized for surface analysis.
-Biosensor with cysteamine (CYSTE) showed increased capture of *Escherichia coli* compared with biosensors with mercaptoproprionic acid (MPA) or cystamine (CYS).